DE-Vol. 35, Rotating Machinery and Vehicle Dynamics
ASME 1991

THE INFLUENCE OF MOUNTING COMPLIANCE AND OPERATING CONDITIONS ON THE RADIAL STIFFNESS OF BALL BEARINGS: ANALYTIC AND TEST RESULTS

M. F. Butner, B. T. Murphy, and R. A. Akian
Rocketdyne
Canoga Park, California

ABSTRACT

Ball bearing stiffness is significantly affected by internal clearance as well as the nature of applied loads and bearing ring mounting compliance. Since their stiffnesses are key to rotor critical speeds, it is important to obtain the most accurate possible radial stiffness prediction for shaft bearings during the machine design analysis process. Quasi-static analysis of spring-preloaded ball bearings predicted reduced radial stiffness when the outer ring is permitted to tilt rather than being assumed restrained from angular deflection. This effect was confirmed experimentally by observing resonant frequencies of a rotor supported on ball bearings of varied internal clearance, mounted with and without spring preloading. Analytic predictions of bearing stiffness are given, and test results presented for comparison.

INTRODUCTION

Radial bearing stiffness is a key factor influencing rotor critical speeds. The abilities to predict accurately and control stiffness are vital to turbomachinery design analyses to assure that undesirable resonances are excluded from operating speed ranges. A prime example of the type of application for which bearing stiffness is a major factor to successful operation is the high pressure oxidizer turbopump (HPOTP) which supplies liquid oxygen to the Space Shuttle Main Engine (SSME) The rotor of the turbopump assembly, shown in cross-section in Figure 1 is supported on two pairs of angular contact ball bearings and operates between approximately 20000 to 30000 rpm. In order to assess the machine's dynamic response over such a large speed range, knowledge of support stiffnesses must be available. To establish confidence in the bearing stiffnesses used in rotordynamic analyses (which traditionally have been analytically predicted), and to confirm the effects of operating conditions, an experimental test series was conducted comparing measured and predicted bearing stiffnesses. The testing cited herein was an extension of a company funded test program initiated in 1982 and reported by Beatty and Rowan (1982). The more recent testing focused on the influence exerted on stiffness of a ball bearing by variations in speed, dynamic radial load, internal clearance, axial preload and mounting compliance both as predicted and experimentally inferred.

This study was conducted as a development task for the Space Shuttle Main Engine (SSME) for the NASA. The subject was the 57 mm bore ball bearing used at the turbine end of the SSME High Pressure Oxygen Turbopump (HPOTP) rotor. The analytic results cited here were calculated using a computer program which was developed by Jones (1960), incorporating a general theoretical treatment of rolling bearings. It calculates the elastic behavior of a system of bearings and their supporting structure under any system of loads. The centrifugal and gyroscopic forces of the rolling elements and the elastic deflections at their contacts are included as well as the interaction of the entire system comprised of the bearings, shaft and housing by the use of influence coefficients. The experimental testing was performed in the Engineering Development Laboratory at the Rocketdyne Division of Rockwell International Corporation in Canoga Park, California in 1988.

SUMMARY

A program was conducted to compare measured radial stiffness of an angular contact ball bearing with analytic stiffness predictions. Altogether, 5 different bearing parameters were investigated for their effect on bearing stiffness. These parameters, and how well the measured stiffness changes correlated with predictions in per cent error, are as follows:

1) rotational speed - 14%, although for a small range
2) dynamic load level - 2.4% (radial deflection = 0.001*bore)

3) axial load - <3% @ < 3550 N (800 lbs) of axial load
- <13% @ > 3550 N (800 lbs) of axial load

4) internal clearance - <7%

5) mount compliance - <5%

Overall, despite significant nonlinear behavior of the test configuration which tend to lower the measured stiffness, predictions were only 5.88% higher on average than measurements, with a standard deviation of 16.0%. The measured results support predictions obtained from a computer code by Jones (1960) used to predict ball bearing stiffness. Considering the limitations in accuracy of the measurement technique, no changes are recommended to the current analysis practice.

BEARING STIFFNESS DEFINITION CONVENTION

The nonlinear relationship between radial deflection and radial load characteristic begs the question of how to define a single stiffness value of a ball bearing for a range of unknown radial loads. The "scaled secant" stiffness used herein is the quotient of the radial load required to produce a radial deflection equal to one thousandth of the bearing bore diameter by that deflection. This convention has been found to give satisfactory results in estimating stiffnesses of ball bearings with compliant mountings for rotordynamic analyses of rocket engine turbopumps, while smoothing variations over a range of loads and deflections. Other definitions of stiffness not used herein but potentially useful in specific instances include:

1. "Secant stiffness": the selected load divided by the deflection resulting from its application. Its value will vary with load.

2. "Slope stiffness": the slope of the force/deflection curve at the selected load. Its value will also vary with load.

FACTORS AFFECTING STIFFNESS

A rolling contact bearing's radial stiffness depends upon its type, size, internal geometry, loading and mounting. Generally, roller bearings are stiffer than ball bearings of similar size, and stiffness can be expected to increase with physical size. Ball bearing stiffness generally increases with reduced internal clearance, closer conformity of raceways to ball, a greater number of smaller balls for a given pitch diameter and contact angle. On the other hand, stiffness is relatively insensitive to ball size changes when internal clearance and pitch diameter are held constant. In addition to the influences of internal geometry, ball bearing stiffness increases with applied axial load, decreases with speed and compliance of its mounting environment. While not a comprehensive study of all factors that affect bearing stiffness, this discussion considers variations in speed, loading, internal clearance, and mounting compliance on the radial stiffness of a specific ball bearing.

TEST BEARING DESCRIPTION

The turbine end bearing of the SSME HPOTP, used as the test bearing for this program, is described in Table 1. In the HPOTP, the bearings are preloaded against each other by springs acting on the outer ring faces (Figure 2). The pair of bearings is mounted in a cartridge of low axial stiffness to permit axial motion of the bearings as a unit. The null position of the cartridge coincides with that established by the balance piston which hydraulically controls rotor axial position when the pump is operating under steady state conditions.

TEST METHOD

The Rocketdyne bearing stiffness tester, Figure 3, is by design a rigid rotor having a center of gravity very close to one bearing. This bearing is designated the test bearing, while the other bearing acts as a slave bearing. In this configuration the first rigid rotor critical speed will be determined primarily by the mass of the shaft (known) and the stiffness of the test bearing (unknown). The test procedure subsequently developed was to slowly vary the speed of the tester to identify its critical speed (as indicated by increased synchronous vibration), and then deduce the bearing stiffness from computer generated curves of critical speed versus test bearing stiffness. In the HPOTP, the bearings are cooled by liquid oxygen; for this testing, however, the bearings were oil lubricated to avoid the operational difficulties that would have arisen from use of a reactive cryogenic coolant.

This procedure is straightforward, but proved difficult to implement, as one additional bearing parameter (i.e., the clearance at the bearing OD, constituting an operational deadband) which strongly influences the critical speed was subject to variations which could not be measured with the instrumentation installed. Deadband lowers the apparent critical speed of a rotor in proportion to the amount of deadband present. This results in what is termed a "nonlinear critical speed" as opposed to the "linear critical speed" that exists with no deadband. Assembly deadbands could of course be measured at uniform ambient temperatures and were on the order of 1E-05m (0.4 mils) radial. Because of the short test durations, the operational deadband was actually variable, increasing or decreasing as the bearing races, balls, lube oil, and housing all changed temperature at their own rates. The actual deadbands experienced during test were then unknown, and in some instances may have been close to zero. When the deadband is zero the resulting critical speed is the "linear critical speed" and is the maximum possible for that particular bearing configuration. Any nonzero value of deadband will lower the critical speed to a value less than the linear critical speed. For example, it can be shown analytically that the measured critical speed can vary 30% or more as a result of changes in deadband.

Through trial and error during the initial phase of the testing, control of temperature was found to be key to obtaining repeatable test results. The lube oil was circulated for extended periods prior to beginning the run to warm it and the hardware so that each run started from as close to the same temperature as possible. In addition, the lube oil was cooled during operation to minimize system temperature ranges.

In analyzing the data, the dependence of the measured stiffness values on deadband variations was minimized as follows. The data from all tests of a given configuration were reviewed to obtain the indicated maximum nonlinear critical speed (as opposed to averaging them). This would yield a measured critical speed as close as

possible to, but not greater than, the linear critical speed. This maximum indicated critical speed was then used with the computer generated curves of linear critical speed versus bearing stiffness to obtain the "measured" stiffness considered to be a lower bound to the actual bearing stiffness.

A nonlinear analysis was performed which predicts the drop in critical speed as a function of deadband, unbalance level, and damping. Since the actual amount of deadband was unknown and could have been close to zero, no attempt was made to correct the measured stiffness for deadband effects. Thus, all measured stiffnesses reported here were obtained in the manner described above.

Figure 4 illustrates and Table 2 lists the predicted and measured stiffnesses found for 56 different configurations of the test bearing, loads and environment. The columns of analytic stiffness values represent the 1 mil deflection per inch of bearing bore secant rule for a deflection/bearing bore ratio of 0.001 previously discussed. Overall, the percentage error between predicted and measured values $(K_p-K_m)/K_m$ averages out to +5.88%. This result in itself is considered quite good given that it was anticipated that the measured values would be lower than predicted (due to deadband effects). The standard deviation of these errors is 16.0%, reflecting the fact that the variable deadband was indeed causing a large degree of variation in the measured critical speeds, as expected.

The observed effects of speed, internal clearance, unbalance, preload, and preload spring compliance are treated separately in the following sections.

ROTOR SPEED

Centrifugal forces that increase with speed cause the individual ball to change position, moving closer to the center of the outer raceway, decreasing the outer contact angle. This outward movement effectively increases the inner race/ball radial clearance. As the inner contact angle increases, the inner ring can be more easily displaced radially, amounting to a decrease in bearing radial stiffness. The effect of speed on the calculated stiffness of the test bearing with maximum and minimum clearance and 4448 N (1000 lb) axial load is shown in Figure 5. The softening effect of speed depends upon the ratio of centrifugal force to axial load, and is therefor lessened at higher axial loads.

To test the theoretically predicted decrease of bearing stiffness with increasing speed two different rotor masses were used. The more massive 31.2Kg (68.66 lbs) rotor would yield a lower critical speed, and thus determine a bearing stiffness measurement at that speed. The lighter 22.42Kg (49.32 lbs) rotor, would yield a critical speed and stiffness measurement at a higher speed. Note however that there are two counteracting effects. The lighter rotor tends to raise the critical speed, but the generally lower stiffness expected at that higher speed tends to lower the critical speed. Table 2 shows the maximum measured critical speeds for all 56 configurations. From these there are 18 heavy/light pairs. The average critical speed increase in going from heavy to light was measured to be 16.4%. The average percentage decrease in stiffness (in going from the lower speed to the higher speed) was measured to be 3.57%, and was predicted to be 5.7%.

UNBALANCE

The load/deflection curve of a preloaded ball bearing is nonlinear due to the effects of internal load distribution and the nature of Hertzian contact deflections. That is, the slope of the load/deflection relation changes with load. To test this experimentally, two different unbalance magnitudes, 3 gm*cm and 9.35 gm*cm (1.2 and 3.68 gram*inches) were employed to yield two different dynamic loading levels. The static loading levels provided by the two rotor weights were not sufficiently different to alter the bearing stiffness detectably.

Among test cases run, there were 22 pairs where unbalance was the only difference (i.e., internal clearance, preload, spring compliance, and rotor weight were the same). The average percentage increase in measured stiffness was 10.4% (s.d.=8.8%). Note however that the measurement of this increased stiffness at the increased unbalance level also occurs at an increased speed, introducing an additional effect on stiffness. In other words, every time a bearing parameter is changed so as to measure its effect on bearing stiffness, there will be an accompanying change in speed which also affects the stiffness.

To nullify this unwanted speed effect, the concept of "normalized stiffness" will be introduced. Every measured stiffness corresponds to its associated speed. As Table 2 shows, resonant speeds used to measure stiffness range from 15,000 to 25,000 rpm. To correct for the effects of the speed range, analytic stiffness values will be used to "normalize" the measured stiffness values to a common speed of 19,000 rpm (this is close to the average measured critical speed). The computed stiffness corresponding to a measured stiffness is divided into a stiffness computed at 19,000 rpm. This quotient is then multiplied by the original measured stiffness to obtain the "normalized" stiffness which is approximately what the measured stiffness would have been had the rotor speed been 19,000 rpm. Normalized stiffness values corresponding to the 19,000 rpm speed are listed in Table 2.

In terms of normalized stiffnesses, the average percentage increase in measured stiffness due to the extra unbalance was then 13.4% (s.d.=9.7%). Although predicted stiffness values are not influenced by unbalance due to the use of the secant stiffness rule, some influence of load amplitude is evident in the test results, which could tend to improve measured stiffness accuracy if different radial deflections are assumed in arriving at the secant stiffness value.

For all the data points obtained with an unbalance of 3 gm*cm (1.2 gm-in), the average percentage error between the measured and predicted stiffnesses (Kp-Km)/Km is 14.95% (s.d.=15.71%). The average measured maximum zero-peak dynamic amplitude divided by the bearing bore (a/B) for these cases is 0.00053. By comparison, at 9.35 gm*cm (3.68 gm-in), the average percentage error for all the data points is 0.4% (s.d.=13.1%). The average maximum dynamic amplitude/bore value here is 0.00083.

These measured data show the dependency of stiffness on dynamic loading level as expressed by the amplitude/bore (a/B) ratio. The 0.001 ratio used to generate the theoretical stiffness predictions does not exactly match either of the loading levels achieved in test. The 0.001 a/B ratio used for turbopump applications was established through experience, and predictions are seen to very closely match

the measured stiffnesses obtained at an a/B of 0.00083. Although these data show that the current prediction methods are quite good, they also suggest that additional work is needed to define analytic methods of obtaining single point stiffness values which yield the best correlation between predicted and measured critical speeds (which will be the subject of a future article).

PRELOAD

That increasing the axial load on an angular contact bearing will result in higher radial stiffness can be appreciated intuitively by considering that the normal forces through the rolling elements will become larger, and therefor a larger radial force is required to displace them in achieving a given radial deflection. To illustrate the influence of axial load and internal clearance, the predicted stiffness as a function of axial load for the test bearing is shown in Figure 6 for the largest and smallest values of internal clearance tested.

Axial preload was the most extensively varied parameter in the test program; data were collected at 7 preload values ranging from 1334 to 4448 N (300 to 1000 lb). Normalized values were used when comparing stiffnesses at different preloads in order to eliminate speed effects. In all, 21 different preload configuration sets were tested ranging from a single preload value to up to 5 preload values per set. To isolate the effect of axial load in the large group of configurations tested (which included two different rotor weights, two unbalances, three internal clearances, and three mounting compliances), pairs of measured stiffnesses at successive preloads were used to compute percentage increases in stiffness per 444.8 N (100 lbs) of increased preload, see Figure 7. The formula used to compute these values is $2(K_{high}-K_{low})/(K_{high}+K_{low})/(P_{high}-P_{low})$. It is seen that the increase in stiffness with preload correlates more favorably for lower than for higher preloads. The measured and predicted percentage increases are within 3.6% for preloads up to 3558 N (800 lb), but above 3558 N (800 lb) the error is as much as 13%. The measured stiffness actually drops, while the predicted values continue to increase. At present the reason for this digression is not known. One possibility is that there is an increase in the deadband effect at high preload values due to increased resistance to outer ring tilt, thus causing lower than normal stiffness measurements.

INTERNAL CLEARANCE

The influence of internal clearance on bearing stiffness can be appreciated by considering an axially preloaded bearing with zero internal clearance. The normal (perpendicular to the contact surfaces) load paths through the individual balls are nearly radial, and bearing radial deflections are composed mostly of elastic contact deflections. If the internal clearance is increased, bearing radial deflections are also composed of motions of the balls out of their original position. These movements, in series with elastic deflections, produce an increase in bearing radial deflection, thus a decrease in bearing radial stiffness.

Three different values of bearing internal clearance, 0.1346, 0.1854, and 0.2362 mm (5.3, 7.3, and 9.3 mils) were tested by assembling the test bearing with ball sets of uniform but different diameters. The measured and predicted stiffness values compare closely. To quantify this, each stiffness delta (for example, as a result of a clearance change from 0.1346 to 0.1854 mm (5.3 to 7.3 mils)) was expressed as a percentage of the mean stiffness for the pair. There are 4 such measured pairs for clearances of 0.1346 and 0.1854 mm (5.3 and 7.3 mil) clearance, and 11 pairs for the 0.1854 and 0.2362 mm (7.3 and 9.3 mil) cases. Table 3 shows the resulting averages of these deltas.

TABLE 3. AVERAGE STIFFNESS DELTA AS A FUNCTION OF INTERNAL CLEARANCE

CLEARANCE PAIR (mm)	NO. SAMPLES	MEASURED AVG. DELTA	PREDICTED AVG. DELTA
.13 to .19	4	-23.7%	-31.3%
.19 to .24	11	-21.2%	-25.8%

For the first group the internal clearance's effect on stiffness is 7.6% over-predicted, and for the second group, about 4.6%.

MOUNTING COMPLIANCE

In a compliantly mounted bearing subjected to combined external radial and axial loads, the distribution of individual ball loads produces a moment about the axis orthogonal to the load direction. In Figure 8, a ball bearing subjected to an axial load along the X axis and a radial load along the Z axis will produce a moment My about the Y axis. Then the outer ring attempts to tilt against the restraint of the mounting. In the case of a spring preloaded ball bearing (Figure 9), this restraint arises from the resisting moments produced by angular deflection of the preload spring and the displaced reaction of the radial load near the bearing outer ring corner contact. As shown in Figure 10, calculated stiffness declines, most rapidly at first, from a totally rigid mounting. It is seen from these graphs that the stiffness of compliantly mounted bearings will be significantly overpredicted if the analysis were based upon an assumption of no tilt. Since most ball bearing outer ring mounting configurations are not totally rigid, the best estimate of effective compliance should be incorporated into stiffness predictions.

In the HPOTP application, the preload springs introduce significant compliance which was factored into bearing stiffness calculations. The effect of preload spring compliance on predicted stiffness of the test bearing is shown in Figure 11, with the two tested compliances marked with circles. The effective compliance with no spring installed is estimated for comparison and marked with a triangle. Spring angular compliance can be determined experimentally, or calculated for a spring with stiffness uniformly distributed around its circumference. For such a spring, angular stiffness can be represented by the expression $(K_s*R_m^2)/2$, where K_s is the axial spring rate and R_m is the spring's mean radius. This assumption is considered valid for the stepped beam springs currently used in the HPOTP, but is probably not applicable to Belleville springs, which may have nonlinear or even unstable angular deflection characteristics. For convenience in bearing stiffness calculation, the tilt resistance of the springs is expressed as a compliance, or the reciprocal of the angular stiffness.

Tests conducted with three different amounts of angular tilt compliance showed that normalized measured data parallels the predictions. The values tested were a) 6.87E-5 radian/N*m (7.76E-6 radian/in-lb), 3.75E-5 radian/N*m (4.25E-6 radian/in-lb) with a stiffer spring installed, and c) a higher angular stiffness with no

preload spring installed, estimated to be 7.08E-6 radian/N*m (8.00E-7 radian/in*lb). On average, the predicted stiffnesses were 11% higher than measured. Nonlinear deadband effects account for part of this overprediction. Also, the two dynamic load levels achieved in test were lower than that used to generate the predictions. By taking this difference into account, the measured and predicted stiffnesses can be shown to be as close as 2.4% on average. To quantify the predicted decrease in stiffness with a more compliant mounting, the stiffness delta (for example, that found as a result of replacing a stiffer spring with a softer one) was expressed as a percentage of the mean stiffness for the pair. There are 10 such measured pairs for the change from stiffer spring to no spring, and 9 pairs for the stiffer to softer springs. Table 4 shows the resulting averages of these deltas.

TABLE 4. AVERAGE STIFFNESS DELTA AS A FUNCTION OF PRELOAD SPRING COMPLIANCE

PRELOAD SPRING GROUP	NO. SAMPLES	MEASURED AVG. DELTA	PREDICTED AVG. DELTA
none to stiff	10	-20.0%	-23.9%
stiff to soft	9	-10.6%	-7.6%

The table shows that the influence of spring compliance on stiffness for the no-spring to stiff-spring is overpredicted by only about 3.9%. The influence of the stiff-spring to soft-spring change is underpredicted by about 3.0%.

CONCLUSIONS

1) The radial stiffness values predicted by the Jones rolling element bearing code are valid if correct input values for operating conditions including mounting compliance are provided. Other codes based upon quasi-static analyses are probably also capable of producing correct stiffnesses, but were not evaluated in the reported effort.

2) Additional testing to increase the understanding of factors influencing bearing stiffness is recommended. Testing could be conducted with the same or similar test equipment, modified in 5 respects:

a) Instrument the bearing carrier with high sensitivity proximity probes to monitor outer race translation and tilt to more accurately assess the extent of bearing deadband interaction, and quantify its influence on bearing stiffness.

b) Include ball orbit (cage) speed measurement, which would permit measurement of operating bearing internal clearance.

c) Locate thermocouples in the housing and bearing outer ring to provide an indication of the operating dead band.

d) Equip the tester with a radial load device to eliminate deadband interaction when desired, and also allow measurement of fixed radial load effects on bearing stiffness.

e) Perform transient impulse testing on the rotating shaft either by using a hammer or mallet, or via a remote control impactor. This will greatly expand testing capability and also improve the accuracy of the measured results.

REFERENCES

Beatty, R.F. and Rowan, B.F., 1982, "Determination of Ball Bearing Dynamic Stiffness". Proceedings of a Workshop, Rotordynamic Instability Problems in High Performance Turbomachinery. NASA Conference Publication 2250, pp 98-104.

Jones, A.B., 1960, "A General Theory for Elastically Constrained Ball and Roller Bearings Under Arbitrary Load and Speed conditions", ASME Trans., Journal of Basic Engineering, 82, Series D, 2, pp 309-320.

TABLE 1. TEST BEARING DESCRIPTION

ITEM	SYMBOL	VALUE	UNITS
BORE	B	.0573	m
OD	D	.1031	m
WIDTH	W	.0195	m
BALL PITCH DIAMETER	E	.0810	m
BALL DIAMETER	d	.0127	m
NUMBER OF BALLS	n	13	-
INNER CURVATURE, r/d	Fi	.55	-
OUTER CURVATURE, r/d	Fo	.53	-
INTERNAL CLEARANCE	Pd	1.346e-4	m
CONTACT ANGLE	BETA	.3660	rad
VARIATIONS			
1)	Pd'	1.854e-4	m
	BETA'	.4305	rad
2)	Pd''	2.362e-4	m
	BETA''	.4870	rad

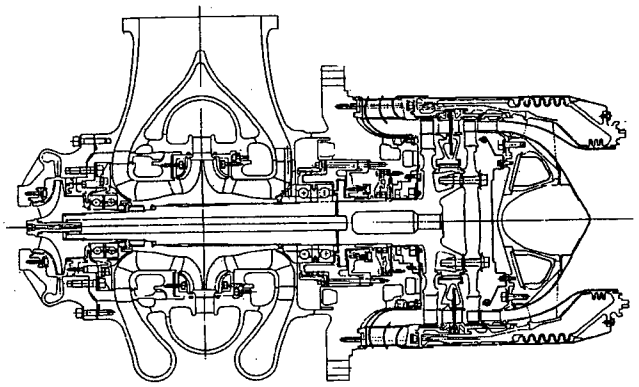

Figure 1. SSME High Pressure Oxidizer Turbopump

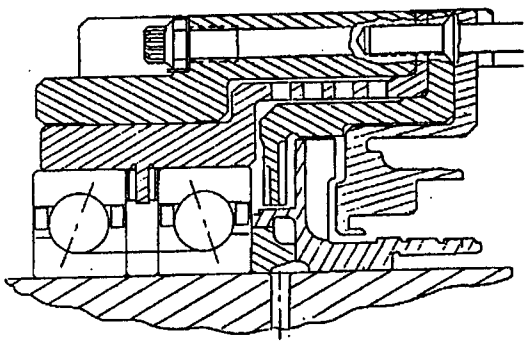

Figure 2. SSME HPOTP turbine end bearing mounting

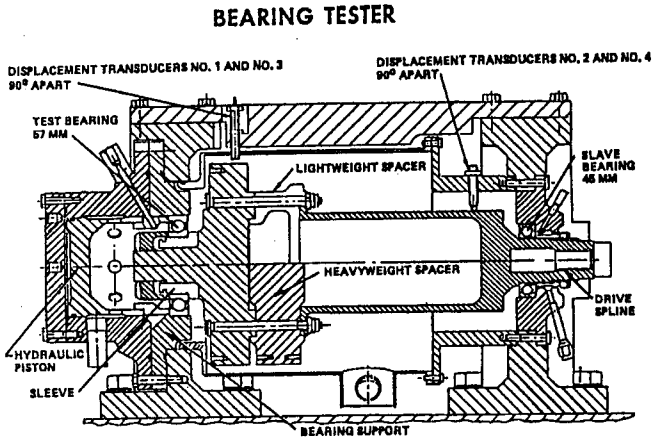

Figure 3. Bearing stiffness tester

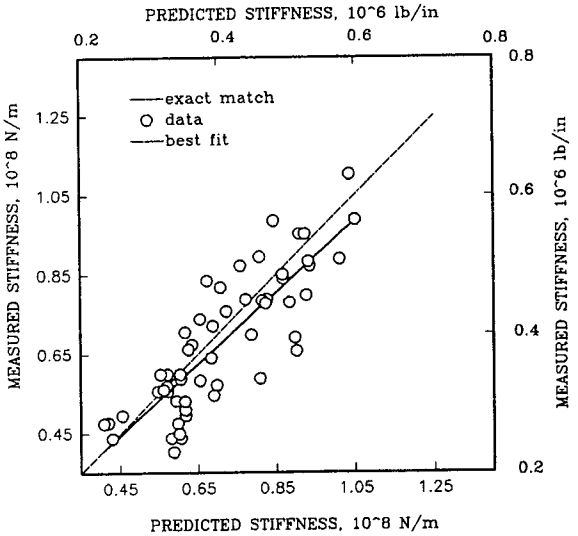

Figure 4. Test result summary: inferred vs predicted stiffness

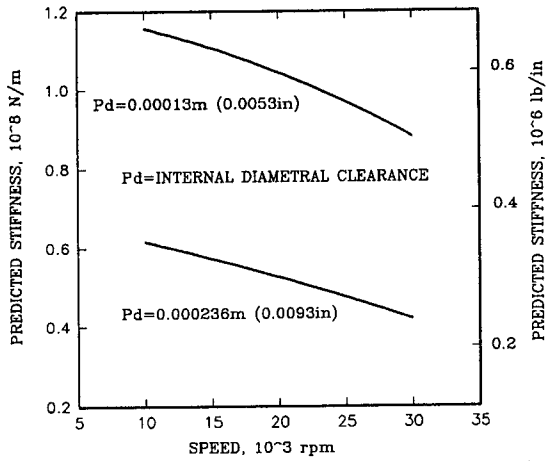

Figure 5. Effect of rotational speed on bearing stiffness

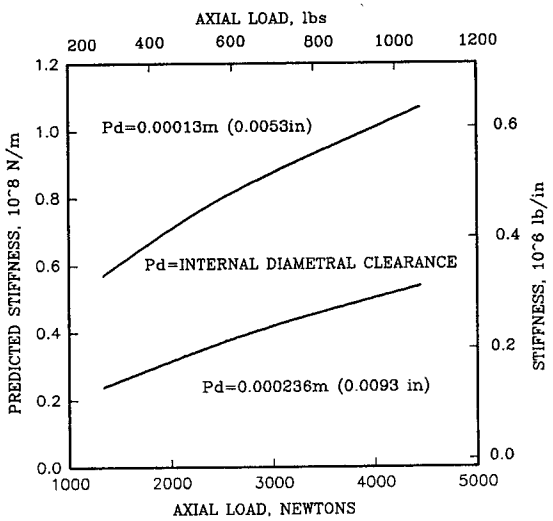

Figure 6. The effect of axial load is shown for the range of internal clearances tested

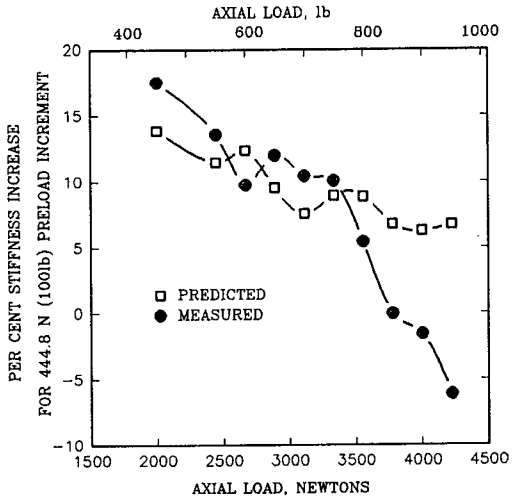

Figure 7. Stiffness trend vs axial load.

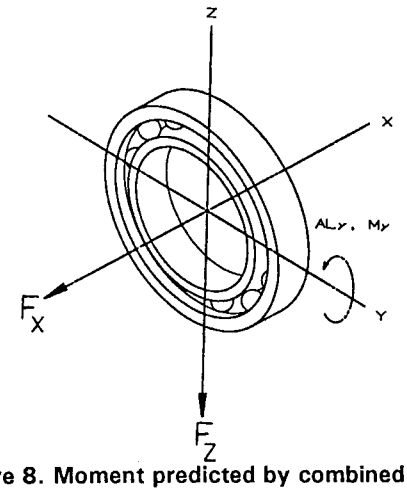

Figure 8. Moment predicted by combined load.

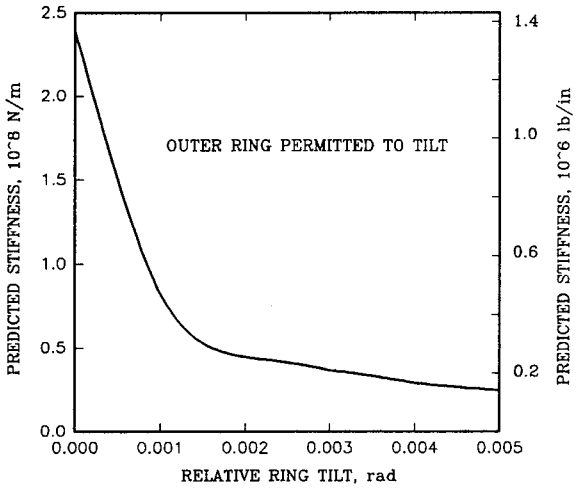

Figure 10. Tilt effect on Stiffness

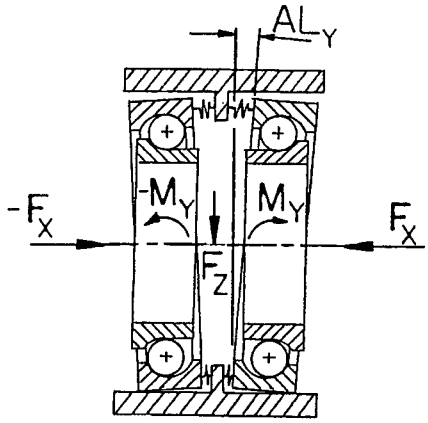

Figure 9. Outer ring tilt

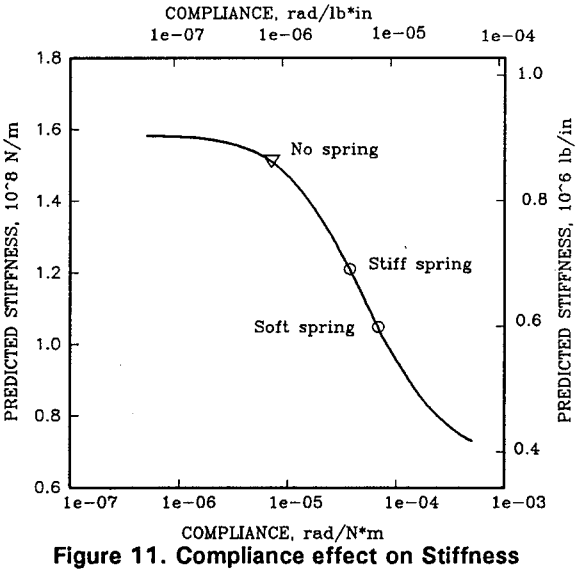

Figure 11. Compliance effect on Stiffness

TABLE 2. BEARING STIFFNESS TESTS

	TEST CONDITION					RESULT	MEASURED		ANALYSIS	
	ROTOR	AXIAL PRE-LOAD	UN-BALANCE	COMPLI-ANCE	Pd DIAMETRAL CLEARANCE	Nc MAX	Kmax N=Nc	Kmax N=19 K	N=N c	N=19 K
CASE	light or heavy	N	gm-cm	1e-6 rad/N*m	mm	rpm	1e8N/m	1e8N/ m	1e8N/ m	1e8N/ m
1	LIGHT	1334	9.35	7.08	.1346	20100	.588	.606	.607	.613
2	LIGHT	2669	9.35	7.08	.1346	24000	.889	.873	1.012	1.057
3	LIGHT	2224	9.35	7.08	.1854	22000	.721	.721	.713	.715
4	HEAVY	2669	9.35	7.08	.1854	19200	.788	.788	.825	.827
5	LIGHT	2224	9.35	7.08	.2362	19600	.556	.573	.548	.553
6	HEAVY	2224	9.35	7.08	.2362	17100	.599	.599	.572	.553
7	HEAVY	3114	9.35	7.08	.2362	18900	.758	.758	.723	.721
8	HEAVY	4003	9.35	7.08	.2362	19700	.839	.839	.868	.881
9	LIGHT	4448	9.35	7.08	.2362	25000	.984	1.002	.844	.957
10	HEAVY	4448	9.35	7.08	.2362	20000	.872	.872	.936	.957
11	LIGHT	1334	9.35	37.62	.1346	19200	.532	.532	.595	.596
12	LIGHT	1334	3.05	37.62	.1346	17500	.438	.426	.606	.596
13	HEAVY	1334	9.35	37.62	.1346	15700	.496	.482	.619	.596
14	HEAVY	1334	3.05	37.62	.1346	15900	.509	.495	.618	.596
15	LIGHT	2669	9.35	37.62	.1346	22750	.780	.825	.884	.931
16	LIGHT	2669	3.05	37.62	.1346	21600	.691	.717	.898	.931
17	HEAVY	2669	3.05	37.62	.1346	19300	.798	.813	.927	.931
18	HEAVY	2669	9.35	37.62	.1346	20700	.952	.969	.909	.931
19	HEAVY	3558	3.05	37.62	.1346	21000	.988	1.004	1.051	1.084
20	HEAVY	3558	9.35	37.62	.1346	21900	1.103	1.139	1.037	1.084
21	LIGHT	2224	3.05	37.62	.1854	19600	.556	.573	.573	.580
22	LIGHT	2224	9.35	37.62	.1854	19800	.569	.585	.571	.580
23	HEAVY	2224	3.05	37.62	.1854	16200	.531	.516	.617	.580
24	HEAVY	2224	9.35	37.62	.1854	17100	.599	.583	.605	.580
25	HEAVY	2669	9.35	37.62	.1854	18700	.739	.739	.655	.651
26	HEAVY	2669	3.05	37.62	.1854	16400	.545	.519	.691	.651
27	HEAVY	3114	9.35	37.62	.1854	19500	.818	.818	.708	.716
28	HEAVY	3558	3.05	37.62	.1854	19200	.788	.805	.773	.776
29	HEAVY	3558	9.35	37.62	.1854	20000	.872	.891	.759	.776
30	HEAVY	4003	3.05	37.62	.1854	19200	.788	.788	.827	.831
31	LIGHT	4448	3.05	37.62	.1854	22800	.784	.848	.815	.881
32	LIGHT	4448	9.35	37.62	.1854	23400	.835	.922	.674	.881
33	HEAVY	4448	3.05	37.62	.1854	17800	.657	.645	.902	.881
34	HEAVY	4448	9.35	37.62	.1854	19800	.850	.866	.866	.881
35	LIGHT	2224	9.35	37.62	.2362	18250	.478	.459	.421	.412
36	LIGHT	2224	3.05	37.62	.2362	17500	.438	.413	.431	.412
37	HEAVY	2224	3.05	37.62	.2362	15700	.496	.459	.457	.412
38	HEAVY	2224	9.35	37.62	.2362	15400	.475	.440	.410	.412
39	HEAVY	3114	9.35	37.62	.2362	17100	.599	.581	.555	.524
40	HEAVY	3114	3.05	37.62	.2362	16600	.560	.543	.563	.524
41	HEAVY	4003	9.35	37.62	.2362	18000	.675	.639	.635	.620
42	HEAVY	4003	3.05	37.62	.2362	16900	.583	.553	.655	.620
43	LIGHT	4448	9.35	37.62	.2362	21800	.706	.744	.617	.662
44	LIGHT	4448	3.05	37.62	.2362	21200	.662	.698	.626	.662
45	HEAVY	4448	9.35	37.62	.2362	17600	.640	.609	.684	.662
46	HEAVY	4448	3.05	37.62	.2362	16750	.572	.537	.698	.662
47	LIGHT	1334	3.05	68.69	.1346	16800	.403	.403	.588	.571
48	LIGHT	1334	9.35	68.69	.1346	17500	.438	.438	.582	.571
49	HEAVY	1334	3.05	68.69	.1346	15400	.475	.475	.599	.571
50	HEAVY	1334	9.35	68.69	.1346	15000	.449	.437	.602	.571
51	LIGHT	2669	3.05	68.69	.1346	20100	.588	.588	.809	.825
52	LIGHT	2669	9.35	68.69	.1346	21700	.698	.713	.787	.825
53	HEAVY	2669	9.35	68.69	.1346	20200	.894	.894	.808	.825
54	HEAVY	2669	3.05	68.69	.1346	19100	.778	.770	.824	.825
55	HEAVY	3558	3.05	68.69	.1346	20100	.883	.899	.933	.950
56	HEAVY	3558	9.35	68.69	.1346	20700	.952	.986	.923	.950